Guided tail modelling for efficient and accurate reliability estimation of highly safe mechanical systems

E Acar
Department of Mechanical Engineering, TOBB University of Economics and Technology, Söğütözü, Ankara 06560, Turkey.
email: acar@etu.edu.tr

The manuscript was received on 14 May 2010 and was accepted after revision for publication on 12 October 2010.

DOI: 10.1177/2041298310392833

Abstract: Classical tail modelling is based on performing a relatively small number of limit-state calculations through Monte Carlo sampling, and then fitting a generalized Pareto distribution to the tail part of the data. The limit-state calculations that do not belong to the tail part are discarded. To reduce the amount of discarded data, this article proposes an efficient tail modelling procedure based on guiding the limit-state evaluations towards the sampling points that have high chances of yielding limit-state values falling into the tail region. The guidance of the limit-state evaluations is achieved through a procedure that utilizes limit-state approximation and distribution fitting. The accuracy of the proposed method is tested through a mathematical problem and four structural mechanics problems, and it is found that the accuracy of reliability estimations can be significantly increased compared to classical tail modelling techniques for the same number of limit-state function evaluations. In addition, it is also found that the improvement in accuracy can be traded off for reducing the number of limit-state evaluations.

Keywords: tail modelling, high reliability, guided Monte Carlo simulations

1 INTRODUCTION

The limit-state function of a mechanical system is usually evaluated through performing computationally expensive finite-element analyses. The simulation techniques such as Monte Carlo method or its advanced variants (e.g. importance sampling [**1**], adaptive importance sampling [**2**], and directional simulation[**3**]) require a large number of limit-state evaluations; hence, they are not suitable for highly safe mechanical systems. Alternatively, the analytical methods such as first-order reliability method (FORM)/second-order reliability method (SORM) are computationally efficient, but their accuracy diminishes as the limit-state function becomes non-linear. In order to overcome the drawbacks of these traditional methods, the techniques based on tail modelling have been successfully used by many researchers including Castillo [**4**], Caers and Maes [**5**], Kim *et al.* [**6**], and Ramu *et al.* [**7**] for reliability assessment of highly safe mechanical systems.

Reliability estimation using tail modelling is based on approximating the tail portion of the cumulative distribution function (CDF) of the limit-state function. Classical tail modelling methods are based on the following procedure [**6**]. First, a set of limit-state evaluations through Monte Carlo simulations (MCS) is performed. Then, a proper threshold value of the CDF is selected that specifies the tail part. Finally, the generalized Pareto distribution (GPD) is fitted to the tail part (i.e. the portion above the threshold value). In this procedure, only the tail part of the limit-state function evaluations is used in finding the parameters of the GPD, while the rest of the data are discarded. The efforts spent for performing limit-state function evaluations that do not belong to the tail part are wasted. Tail modelling can be performed more efficiently if the amount of wasted data is reduced.

This article proposes an efficient tail modelling procedure based on guiding the limit-state evaluations towards the sampling points that have high chances of producing limit-state values falling into the tail region. Therefore, the proposed method is named as the *guided* tail modelling. The guidance of the limit-state evaluations is achieved through a procedure that utilizes the univariate dimension reduction (UDR) method of Rahman and Xu [**8**] and distribution fitting using extended generalized lambda distributions (EGLD). The unique contribution of the article is that the large amount of discarded data, which is

the by-product of the tail models presented in the previous studies, is significantly reduced through guided tail modelling, thereby leading to more efficient and more accurate reliability estimation of highly safe mechanical systems.

The article is organized as follows. Section 2 presents an overview of classical tail modelling. The proposed guided tail modelling procedure is outlined in section 3, and the method is demonstrated with a well-known beam design problem in section 4. Four additional example problems are provided in section 5. The limitations of the proposed method are discussed in section 6, followed by concluding remarks given in section 7.

2 OVERVIEW OF CLASSICAL TAIL MODELLING

The fundamental idea of the tail modelling technique is based on the property of tail equivalence. Two distribution functions $F(x)$ and $G(x)$ are called tail equivalent if the following condition is satisfied [**9**]

$$\lim_{x\to\infty}\frac{1-F(x)}{1-G(x)}=1 \tag{1}$$

Here, the tail model of $F(x)$ is used for approximating the upper (or lower) tail of $G(x)$. This approach does not take into account the central behaviour of the distribution. Rather, it focuses on the upper or lower tail behaviour, which fits for the purpose of reliability analysis of highly safe mechanical systems.

Now, consider the limit-state function $y(x)$, where x is the vector of random variables. For a large threshold value of y_t (see Fig. 1), the region above the threshold (i.e. the tail portion) can be approximated using GPD. The GPD approximates the conditional excess distribution of $F_z(z)$, where $z=y-y_t$, via

$$F_z(z)=\begin{cases}1-\left\langle 1+\dfrac{\xi}{\sigma}z\right\rangle_+^{-1/\xi} & \text{if } \xi\neq 0\\ 1-\exp\left(-\dfrac{z}{\sigma}\right) & \text{if } \xi=0\end{cases} \tag{2}$$

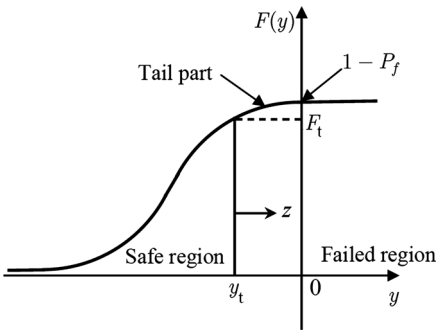

Fig. 1 Tail modelling concept

where $\langle A\rangle_+=\max(0,A)$, $z\geqslant 0$, and $F_z(z)$ is the GPD with shape and scale parameters ξ and σ, respectively, which need to be determined.

The conditional excess distribution can be related to the cumulative distribution $F(y)$ through

$$F_z(z)=\frac{F(y)-F(y_t)}{1-F(y_t)}=\frac{F(y)-F_t}{1-F_t} \tag{3}$$

Then, $F(y)$ above the threshold (i.e. $y\geqslant y_t$) is expressed in terms of the conditional excess distribution, $F_z(z)$, via

$$F(y)=F_t+(1-F_t)F_z(y-y_t) \tag{4}$$

Once the CDF $F(y)$ is obtained, the probability of failure, P_f, can be estimated from reference [**6**]

$$P_f=1-F(y=0)=(1-F_t)\left\langle 1-\frac{\xi}{\sigma}y_t\right\rangle_+^{-(1/\xi)} \tag{5}$$

The reliability index can be calculated from

$$\beta=\Phi^{-1}(1-P_f) \tag{6}$$

where Φ is the CDF of a standard normal random variable.

The classical tail modelling methods are based on the following three-step procedure.

1. N samples of the limit-state function $y(\boldsymbol{x})$ are generated through MCS (or Latin hypercube sampling). In structural mechanics problems, the samples of the input random variables, x, are first generated from the given distribution types. The samples of the random limit-state function are then calculated through the structural analysis (usually through computationally expensive finite-element analysis).
2. A threshold value, y_t, is selected from the distribution of the limit-state function $y(\boldsymbol{x})$. The appropriate value y_t, that is, the specification of the beginning of the upper tail, has been the subject of extensive research, and empirical values for it have been proposed [**5**, **10**, **11**]. For instance, Hasofer [**11**] suggested using $N_t\approx 1.5\sqrt{N}$, where N_t is the number of data that belongs to the tail part, and N is the total number of data.
3. The shape and scale parameters in the GPD (i.e. ξ and σ), are estimated by fitting the tail model with the empirical CDF. Two methods are commonly used for this purpose: the maximum likelihood (ML) method and the least square (LS) method. The reader is referred to reference [**12**] for details of these two methods.

3 GUIDED TAIL MODELLING

As noted earlier, the classical tail modelling uses only the tail part of the data in estimating the GPD parameters, while the other data are discarded. If there exists a computationally inexpensive approximate model for the limit-state function and the threshold value y_t is known, then limit-state evaluations can be guided towards sampling points that have high chances of yielding limit-state values falling into the tail region. Therefore, the tail modelling can be performed more efficiently since the amount of wasted data can be reduced. For instance, the following simple procedure can be employed. First, a large number of potential sampling points are generated via MCS. Next, the approximate value of the limit-state function is computed for all these potential sampling points. Then, the points with approximate limit-state values larger than the threshold y_t are stored. Finally, the actual limit-state function calculations are performed only for these stored points since they have high chances of producing actual limit-state values in the tail region.

In this study, the approximate model for the limit-state function is constructed through an additive decomposition technique used in the UDR method. The threshold value y_t is estimated via an efficient distribution fitting technique that blends UDR and EGLD. Before proceeding with outlining the proposed tail modelling procedure, the brief details of UDR and EGLD are provided below.

3.1 Limit-state function approximation using UDR method

As part of the UDR method, an additive decomposition technique is used such that a multi-dimensional limit-state function $y(\mathbf{X})$ is approximated using multiple uni-dimensional functions as [**8**]

$$\hat{y}(\mathbf{X}) = \sum_{j=1}^{N} y_j^u(X_j) - (N-1)y_0 \tag{7}$$

where each term in the summation, y_j^u, is a uni-dimensional function that depends on the jth random variable, X_j, that is

$$y_j^u(X_j) = y(\mu_1, \ldots, \mu_{j-1}, X_j, \mu_{j+1}, \ldots, \mu_N) \tag{8}$$

whereas y_0 is the value of $y(\mathbf{X})$ calculated at the mean values of all the random variables, $\mu_j, j = 1, \ldots, N$

$$y_0 = y(\mu_1, \ldots, \mu_N) \tag{9}$$

For the uni-dimensional functions, $y_j^u(X_j)$, metamodels can be constructed using a small number of simulations. A quadratic polynomial in one dimension has three coefficients, and so five sampling points may provide a good approximation for y_j^u. For highly non-linear functions, however, the number of sampling points may need to be increased. The locations of the sampling points can be determined by using the moment-based quadrature points proposed by Rahman and Xu [**8**]. If the random variable X_j is normally distributed, the moment-based quadrature method produces Gauss–Hermite points. When five points are used for each uni-dimensional function, y_j^u, overall $4N + 1$ sampling points are needed (for symmetric distributions), since the third sampling point for all y_j^u is equal to y_0.

3.2 Distribution fitting via UDR method and EGLD

The statistical moments of the limit-state function can be calculated efficiently using the UDR method. After the first four moments of the limit-state function are calculated, these moments can be matched with the moments of an EGLD, so that the distribution parameters of the fitted EGLD are assessed. The reader is referred to references [**13**] to [**16**] for more information regarding the EGLD and finding its distribution parameters using the statistical moments.

After the distribution parameters of the EGLD are found, the threshold value y_t can easily be estimated from the inverse CDF of the fitted EGLD via

$$y_t = F_{\text{EGLD}}^{-1}(F_t) \tag{10}$$

where F_{EGLD} is the CDF of the fitted EGLD, and F_t is the selected threshold CDF value. For details of distribution fitting via UDR and EGLD, the reader is referred to Acar *et al.* [**17**], where UDR method and EGLD are used together for reliability prediction of mechanical systems with moderate reliability levels (i.e. reliability $\leqslant$0.99), and named this procedure of reliability assessment as UDR + EGLD.

3.3 Guided tail modelling procedure

After briefly describing how the limit-state function is approximated and the threshold value y_t is estimated, the proposed guided tail modelling procedure can now be outlined as follows.

1. Perform $4n + 1$ limit-state function (y) evaluations, where n is the number of random variables. As noted earlier in section 3.1, if y is highly non-linear, more function evaluations such as $6n + 1$ or $8n + 1$ may be needed.
2. Fit uni-dimensional metamodels using $4 + 1 = 5$ points corresponding to each random variable.
3. Use UDR method to calculate the first four statistical moments of the limit state.

4. Approximate the distribution of the limit state via EGLD, and estimate the threshold value, y_t, corresponding to a pre-specified threshold value of F_t (here $F_t = 0.95$ is used).
5. Generate N sampling points, compute approximate limit-state function values at the sampling points via UDR, and store the ones greater than y_t. If UDR and EGLD did not include any errors, exactly $0.05N$ points for $F_t = 0.95$ would be stored. If necessary, additional points can be created or extra points can be deleted in a proper way.
6. For the stored sampling points, compute the actual limit-state function values, perform the tail modelling (i.e. fit GPD), and calculate the probability of failure.

Note that in the guided tail modelling procedure, the use of $4n + 1$ points, the use of EGLD for distribution fitting or the use of $F_t = 0.95$ are not restrictive, but a personal choice. These values can be altered by the specialist.

3.4 Comparison of the guided tail modelling to the classical tail modelling

In classical tail modelling, first a random sampling or Latin hypercube sampling is performed over the input random variables. The number of samples generated is limited due to restrictions in resources and time. Assume that 1000 samples are generated. Then, the actual limit-state evaluations are performed for all these 1000 samples. Then, based on a pre-selected tail threshold limit (e.g. 95 per cent), the threshold value of the limit-state, y_t, is computed. The limit-state values are sorted and the 950th value gives the threshold value of the limit-state. Then, 951st through 1000th values are used in order to fit a GPD (see equation (2)). Finally, the probability of failure is computed using the fitted GPD (see equation (5)).

In the proposed guided tail method, first $4n + 1$ samples are generated based on the UDR technique, where n is the number of random variables. These samples are used for two purposes:

(a) predicting the threshold value y_t;
(b) constructing a UDR-based metamodel.

Since the pre-selected value of the tail threshold limit is usually not larger than 95 per cent, UDR + EGLD predict the threshold value of the limit-state, y_t, quite accurately. Once y_t is predicted, the UDR-based metamodel is used as follows. First, a very large number of sampling points are generated. For instance, if the number of envisioned limit-state evaluations is 1000, then 20 000 sampling points are generated. Note here that actual limit-state evaluations are not performed yet. Then, the UDR-based metamodel is used for identifying the sample points that are highly likely to yield limit-state values falling into the tail region. The actual limit-state function evaluations are performed for these guided (or selected) points. Finally, the actual limit-state values above the threshold value of the limit-state, y_t, are used in order to fit GPD, and compute the reliability.

Note that the UDR-based metamodels are intended to do classification (whether falling into the tail region) rather than doing regression, and therefore the predictive accuracy of UDR-based metamodels may not be good. Therefore, if the UDR-based metamodels are used within a Monte Carlo setting, this may result in very large errors in reliability estimations. Even if the predictive accuracy of a UDR-based metamodel is acceptable, one may still have large errors in reliability estimations, because it has been shown that even very small errors in limit-state function metamodels may result in large errors in reliability estimations [**18**].

4 DEMONSTRATION OF THE GUIDED TAIL MODELLING PROCEDURE

To illustrate the proposed approach, the well-known cantilever beam design problem is considered. This problem was first introduced by Wu *et al.* [**2**] and has been analysed by many researchers [**7**, **19**, **20**]. The cantilever beam depicted in Fig. 2 has two failure modes: stress failure and excessive displacement. The minimum weight design is sought by varying the width w and thickness t of the beam. The applied loads F_X and F_Y as well as the elastic modulus E and yield strength R are random. The random variables are normally distributed with mean and coefficient of variation values as listed in Table 1. The beam width w and thickness t are modelled as deterministic variables.

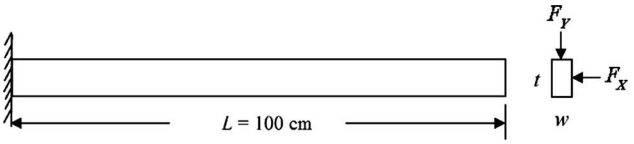

Fig. 2 Cantilever beam: geometry and loading

Table 1 Mean and coefficient of variation of the random variables for Wu's beam problem

Random variable	Mean	Coefficient of variation (%)
F_X (N)	500	20
F_Y (N)	1000	10
E (MPa)	2900	5
R (MPa)	400	5

Note that all random variables follow normal distribution.

The limit-state functions corresponding to stress failure mode can be written as

$$y_s = R - \left(\frac{600}{wt^2}F_Y + \frac{600}{w^2t}F_X\right) \tag{11}$$

Similarly, the limit-state functions corresponding to displacement failure mode can be written as

$$y_d = D_0 - \frac{4L^3}{Ewt}\sqrt{\left(\frac{F_Y}{t^2}\right)^2 + \left(\frac{F_X}{w^2}\right)^2} \tag{12}$$

where the beam length L is taken as 100 cm and the critical displacement D_0 is set to 2.2535 cm.

The minimum weight design of the beam with reliability indices of both failure modes having a target value of 3.0 was solved by Wu *et al.* [**2**] using FORM. They found the optimum design with the geometric features $w = 2.4494$ cm, $t = 3.8884$ cm, and reported the reliability indices of the stress and displacement failure modes as 3.0071 and 3.0097, respectively. To check the accuracy of FORM solution, an MCS is performed with 10^8 samples in this study and the reliability indices for stress and displacement failure modes are computed as 3.007 and 2.996, respectively. These reliability index values are used while assessing the accuracy of the guided tail modelling. To demonstrate the guided tail modelling procedure, reliability index estimation of the displacement failure mode (the stress failure mode is much simpler) is performed. The results are provided in a step-by-step manner as follows:

Step 1: Perform $4n + 1$ limit-state function evaluations.

The limit-state function of the displacement failure mode includes three random variables, namely F_X, F_Y, and E (hence, $n = 3$). Therefore, $4n + 1 = 13$ limit-state evaluations are performed as listed in Table 2.

Table 2 $4n + 1$ limit-state function evaluations needed for one-dimensional metamodel fitting and statistical moment computations via UDR for Wu's beam problem

Simulation number	F_X (N)	F_Y (N)	E (MPa)	$-y_d$
1	500	1000	2900	−5.168
2	785.7	1000	2900	−0.935
3	635.6	1000	2900	−3.227
4	364.4	1000	2900	−6.910
5	214.3	1000	2900	−8.447
6	500	1285.7	2900	−3.838
7	500	1135.6	2900	−4.560
8	500	864.4	2900	−5.727
9	500	714.3	2900	−6.280
10	500	1000	3314	−7.502
11	500	1000	3097	−6.275
12	500	1000	2703	−4.061
13	500	1000	2486	−2.834

These limit-state values will be used for fitting metamodels for one-dimensional functions in the UDR, and calculating the first four statistical moments of the limit-state function. Since the upper tail is modelled, the negative values of the limit-state function in equation (12) are used.

Step 2: Fit uni-dimensional metamodels using five points for each random variable.

To relate the displacement limit-state function to the random variables, quadratic response surface approximations are used. For the case of very non-linear limit states, other types of metamodels such as Kriging or radial basis functions can be used. The uni-dimensional metamodel for F_X is constructed using simulation numbers 1–5. The constructed metamodel is shown in Fig. 3(a). Similarly, uni-dimensional metamodels are constructed for F_Y using simulation numbers 1, and 6–9, and for R using simulation numbers 1, and 10–13. The metamodels for F_Y and E are depicted in Figs 3(b) and (c).

Step 3: Use UDR method to calculate the first four statistical moments of the limit state.

UDR method of Rahman and Xu [**8**] is used for calculating the first four moments of the limit-state function. The computed moments are provided in Table 3. The displacement failure limit-state function, equation (12), is a non-linear function, and so the mean, standard deviation, skewness, and kurtosis values are calculated through MCS with a million sampling points. Table 3 presents a comparison of the mean, standard deviation, skewness, and kurtosis values calculated through UDR and through MCS. Notice that UDR estimations are quite accurate.

Step 4: Approximate the distribution of the limit-state function via EGLD, and estimate the threshold value y_t, corresponding to a pre-specified threshold value of F_t.

The computed statistical moments of the limit-state function are used for approximating the distribution of the limit-state function through EGLD. The fitted EGLD is compared with the empirical PDF in Fig. 4. The empirical PDF is obtained through MCS with a million samples. Notice that the fitted CDF matches well with the empirical PDF. Using the fitted distribution, the threshold value y_t, corresponding to $F_t = 0.95$, is computed as $y_t = -2.334$. The threshold value computed through MCS with a million sampling points is found as $y_t = -2.339$. Notice that the UDR prediction is very close.

Step 5: Generate N sampling points, approximate limit-state function values at the sampling points via UDR, and store the ones greater than y_t.

Here, it is assumed that the number of limit-state function evaluations is limited to 1000 due to the

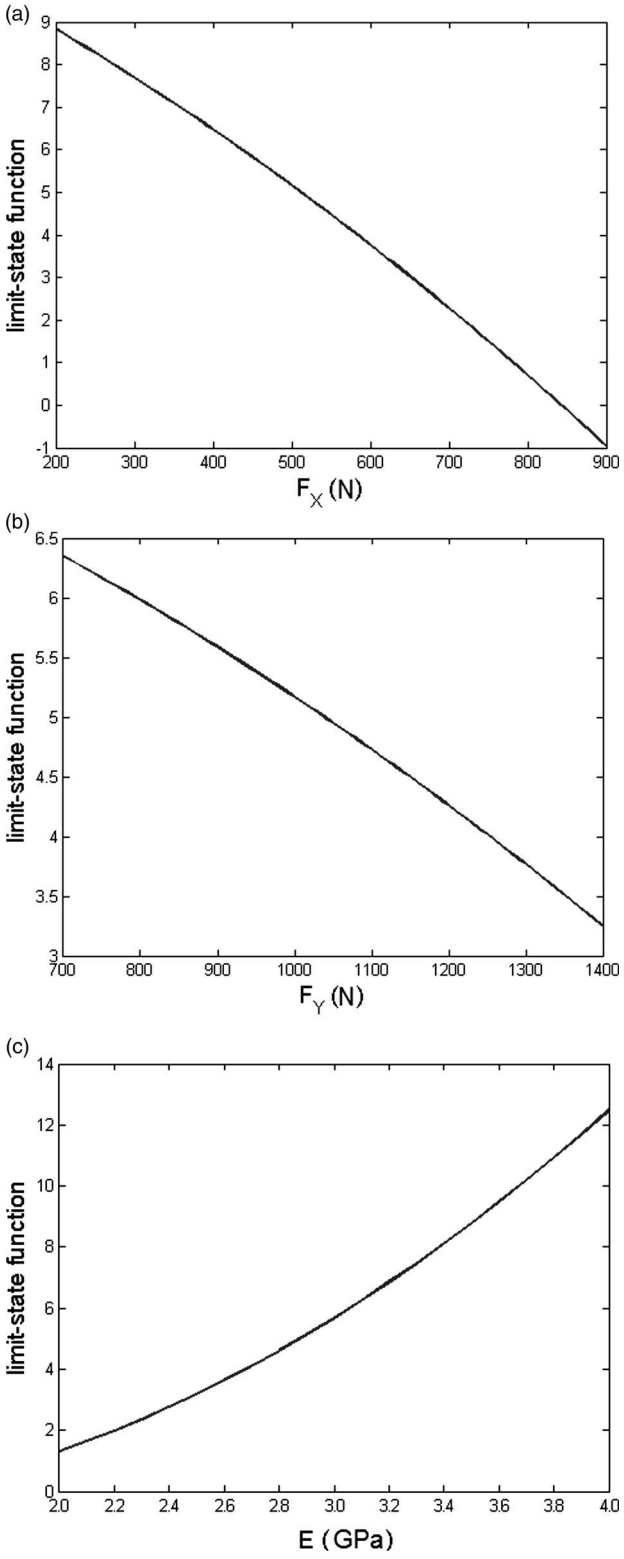

Fig. 3 Metamodels for the responses in the displacement limit-state function of Wu's beam problem: (a) metamodel for F_X; (b) metamodel for F_Y; and (c) metamodel for E

restrictions on time and computational resources. Therefore, $0.05N = 1000$, so 20 000 samples are generated. If UDR and EGLD approximations did not include any errors, exactly 1000 points would be stored. Here, it is found that 988 points are stored on average. Combined with the earlier 13 simulations (performed for the UDR), the total number of function evaluations is 1001.

Table 3 Statistical moments of y_d: actual values vs. the values computed through UDR for Wu's beam problem

	Mean	Standard deviation	Skewness	Kurtosis
UDR	−5.0997	1.638	0.141	2.985
MCS	−5.0994	1.640	0.094	2.991

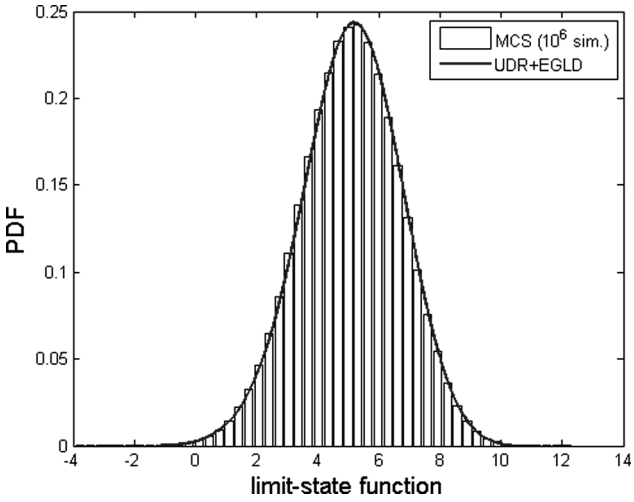

Fig. 4 Tail modelling for limit-state function for the displacement failure of Wu's beam problem

Step 6: For the stored sampling points, compute the actual limit-state function values, perform the tail modelling (i.e. fit GPD), and calculate the probability of failure.

For the stored 988 points, actual limit-state function evaluations are performed. The fitted GPD and the actual normal distribution are depicted in Fig. 5. It is seen that the constructed GPD is in good match with the empirical distribution obtained through MCS with sample size of 10^6. Having this fitted GPD, the probability of failure and reliability index can be calculated using equations (5) and (6). The reliability index is computed as 2.971, while the actual value of the reliability index is 3.007. Therefore, the error in reliability index estimation is 1.2 per cent.

Note that the results reported above are computed using a particular sample. To reduce the effect of random sampling, the whole procedure is repeated 100 times with different samples, and the mean absolute error in reliability index estimation is computed. In addition, the classical tail modelling techniques with 1000 samples and a threshold value of 0.95 are

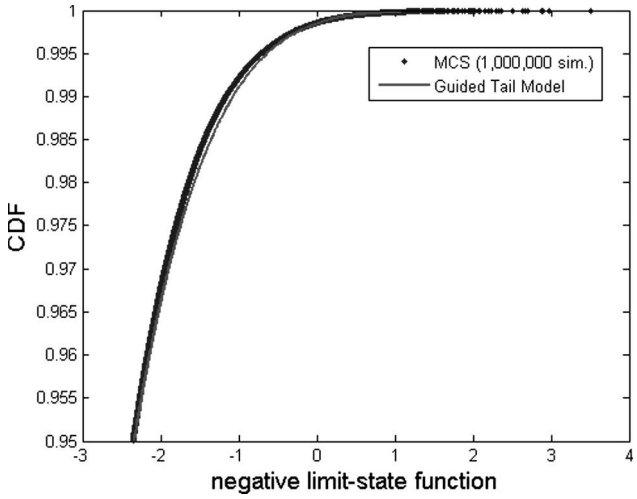

Fig. 5 Tail modelling for limit-state function for the displacement failure of Wu's beam problem

Table 4 Comparing the accuracies of classical tail modelling and guided tail modelling for Wu's beam problem for target reliability index of 3.0

Failure mode	% Error in classical tail modelling estimations			% Error in guided tail modelling
	ML	LS	Average	
Stress	7.2	9.2	7.1	1.3
Displacement	7.8	10.7	8.0	1.5

employed for 100 times with different samples and the mean absolute error is computed. The comparison of the accuracies of the classical tail modelling techniques and the guided tail modelling is given in Table 4. Notice in Table 4 that the reliability estimations for both the stress failure mode and the displacement failure mode are provided. While the classical tail modelling techniques lead to errors of 7–11 per cent, the error of the guided tail modelling is smaller than 2 per cent.

To investigate the effect of the increased reliability index, the beam design problem is solved for target reliability index values of 3.5 and 4.0. First, FORM is used for computing the optimum values of the width and the height of the beam, and then MCS with a sample size of 10^8 are performed to compute the reliability indices more accurately. The beam designs and corresponding reliability indices are provided in Table 5.

Table 6 Comparing the accuracies of classical tail modelling and guided tail modelling for Wu's beam problem for target reliability index of 3.5

Failure mode	% Error in classical tail modelling estimations			% Error in guided tail modelling
	ML	LS	Average	
Stress	12.5	16.4	11.0	2.4
Displacement	13.8	10.7	14.5	3.9

Table 7 Comparing the accuracies of classical tail modelling and guided tail modelling for Wu's beam problem for target reliability index of 4.0

Failure mode	% Error in classical tail modelling estimations			% Error in guided tail modelling
	ML	LS	Average	
Stress	13.5	18.3	11.8	5.7
Displacement	19.1	22.4	16.2	13.7

Notice that the FORM predictions are very close to MCS results.

The comparisons of the accuracies of the classical tail modelling techniques and the guided tail modelling for reliability indices of 3.5 and 4 are provided in Tables 6 and 7, respectively. As seen from these tables, the accuracy of guided tail modelling is much better than those of the classical tail models for about the same number of limit-state function evaluations.

The improvement in the accuracy of reliability index estimations through guided tail modelling can be traded off for reducing the number of limit-state evaluations. Instead of increasing the accuracy of reliability index estimations compared to those of the classical tail modelling, the number of limit-state evaluations can be reduced without jeopardizing the accuracy. Tables 8 and 9 compare the accuracies of guided tail modelling with 100 envisioned limit-state evaluations to the accuracies of the classical tail modelling with 1000 limit-state evaluations for various reliability index values. The actual number of limit-state evaluations is slightly different from that of the envisioned number of limit-state evaluations due to errors in UDR-based metamodels. Tables 8 and 9 show that the accuracy of the guided tail modelling is better than that of the classical tail modelling, even though the number of limit-state evaluations is about an order of magnitude smaller.

Table 5 Beam design and corresponding reliability indices

Target reliability index	Width (cm)	Height (cm)	Stress reliability index (FORM)	Displacement reliability index (FORM)	Stress reliability index (MCS)	Displacement reliability index (MCS)
3.5	2.5135	3.9136	3.5	3.668	3.5	3.654
4.0	2.5786	3.9400	4.0	4.349	4.004	4.341

Table 8 Reduced actual limit-state evaluations via guided tail modelling for stress failure mode of Wu's beam problem

	Guided tail modelling			Classical tail modelling
Reliability index	Envisioned number of limit-state evaluations*	Actual number of limit-state evaluations*	% Error	% Error with 1000 limit-state evaluations†
3.0	100	99	4.4	7.1
3.5	100	100	9.8	11.0
4.0	100	99	12.6	16.2

*Note that an additional 13 limit-state evaluations are performed for UDR prior to tail modelling.
†The smallest of ML, LS, and average is used for comparison (see Tables 4, 6, and 7).

Table 9 Reduced actual limit-state evaluations via guided tail modelling for displacement failure mode of Wu's beam problem

	Guided tail modelling			Classical tail modelling
Reliability index	Envisioned number of limit-state evaluations*	Actual number of limit-state evaluations*	% Error	% Error with 1000 limit-state evaluations†
2.97	100	102	5.1	7.8
3.67	100	102	10.1	10.7
4.35	100	101	15.7	16.2

*Note that an additional 13 limit-state evaluations are performed for UDR prior to tail modelling.
†The smallest of ML, LS, and average is used for comparison (see Tables 4, 6, and 7).

The guided tail modelling reliability predictions are dependent on the selected threshold value F_t for the CDF. The sensitivity of the guided tail modelling predictions to F_t is investigated. Table 10 presents the comparison of guided tail modelling predictions using $F_t = 0.90$ and $F_t = 0.95$ for Wu's beam problem for various reliability levels. Table 10 shows that the use of $F_t = 0.95$ leads to more accurate reliability predictions than $F_t = 0.90$, while the guided tail predictions using $F_t = 0.90$ are still more accurate than those of the classical tail modelling (compare Table 10 to Tables 4, 6, and 7). Note that with $N = 1000$ samples, the number of samples in tail region N_t proposed by Hasofer [**11**] is $N_t \approx 1.5\sqrt{N} = 47.4$, which is close to 50 samples corresponding to the use of $F_t = 0.95$.

5 RESULTS AND DISCUSSIONS

This section provides a mathematical example with a highly non-linear limit-state function and two more mechanics problems to evaluate the efficiency of the guided tail modelling. The comparisons of the results of the all example problems and related discussions are provided in this section.

5.1 Additional example 1: a highly non-linear limit-state function

This mathematical example problem is provided to investigate the effectiveness of the proposed method when the limit-state function is highly non-linear. The well-known Goldstein–Price function [**21**] is used for defining the limit-state function as

$$Y = y_{\text{crit}} - y(x_1, x_2) \tag{13}$$

where the Goldstein–Price function is

$$\begin{aligned} y(x_1, x_2) = {} & [1 + (x_1 + x_2 + 1)^2(19 - 14x_1 \\ & + 3x_1^2 - 14x_2 + 6x_1x_2 + 3x_2^2)] \\ & \times [30 + (2x_1 - 3x_2)^2(18 - 32x_1 \\ & + 12x_1^2 + 48x_2 - 36x_1x_2 + 27x_2^2)] \end{aligned} \tag{14}$$

Here, the variables x_1 and x_2 are taken as random variables with standard normal distributions. Figure 6 depicts the highly non-linear behaviour of the Goldstein–Price function when the random variables take values within the range of ± three standard deviations away from the mean values.

The value of y_{crit} in equation (13) is adjusted to obtain various values of reliability indices as listed in Table 11. The reliability indices in the second column of Table 11 are computed via MCS with a sample size of 10^8. The comparison of the reliability estimation of the classical tail modelling techniques and guided tail

Table 10 Comparison of guided tail modelling predictions using different threshold values F_t for Wu's beam problem

Stress failure mode			Displacement failure mode		
Reliability index	% Error in guided tail modelling using $F_t = 0.90$	% Error in guided tail modelling using $F_t = 0.95$	Reliability index	% Error in guided tail modelling using $F_t = 0.90$	% Error in guided tail modelling using $F_t = 0.95$
3.0	1.8	1.3	2.97	2.2	1.5
3.5	4.3	2.4	3.67	6.5	3.9
4.0	11.2	5.7	4.35	16.6	13.7

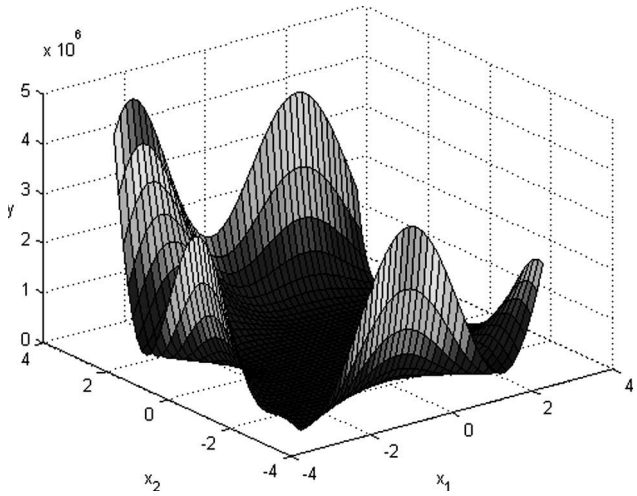

Fig. 6 Variation of the Goldstein–Price function over $x_1, x_2 \in [-3, 3]$

modelling is also provided in Table 11. For the classical tail models, the threshold value of $F_t = 0.95$ is used and 1000 limit-state calculations are performed. For the guided tail modelling, two scenarios are considered. First, the envisioned number of limit-state evaluations is kept at 1000, and it is found that the accuracies of the reliability estimations are improved compared to classical tail modelling. Second, the envisioned number of limit-state evaluations is reduced to 100, and it is observed that the accuracy of reliability index estimations is not jeopardized much.

Note that the reliability estimations could also be performed by using only the UDR and EGLD combination, without performing any additional tail modelling. After the EGLD is fitted, the reliability could easily be estimated [**17**]. The last column of Table 11 shows the reliability index estimations by using UDR + EGLD. It is seen that the UDR + EGLD predictions are not accurate as the limit-state function is highly non-linear.

5.2 Additional example 2: eight-variable I-beam design problem

In this example, a simply supported I-beam (see Fig. 7) under a concentrated load as discussed in reference

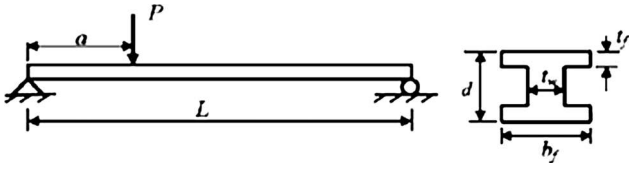

Fig. 7 Cross-section and loading on the eight-variable I-beam

Table 12 Mean and standard deviation values of the random variables for the eight-variable beam problem

Random variable	Mean; standard deviation
P	6070; 200
L	120; 6
a	72; 6
S	170000; 4760
d	2.3; 1/24
b_f	2.3; 1/24
t_w	0.16; 1/48
t_f	0.26; 1/48

Note that all random variables follow normal distribution.

[**22**] is examined. The limit-state function for this problem is formulated as the difference between the strength, S, and load effect in terms of maximum normal stress, σ_{max} due to bending given by

$$Y = S - \sigma_{max} \tag{15}$$

where

$$\sigma_{max} = \frac{Pa(L-a)d}{2LI}; \quad I = \frac{b_f d^3 - (b_f - t_w)(d - 2t_f)^3}{12} \tag{16}$$

In this problem, there are eight random variables following normal distribution with mean and standard deviation values provided in Table 12. The main motivation for analysing this problem is to investigate the effects of increasing the number of input random variables on the effectiveness of the guided tail modelling.

With the values used in the original problem definition, the reliability index for the beam is about 1.132, which is small for this study. Higher values of

Table 11 Comparing the accuracies of classical tail modelling and guided tail modelling for the highly non-linear limit-state problem for various target reliability index values

y_{crit}	Reliability index	% Error in classical tail modelling (1000 simulation)			% Error in guided tail modelling (1000 simulation)	% Error in guided tail modelling (100 simulation)	% Error in UDR + EGLD
		ML	LS	Average			
3×10^6	2.740	2.4	4.4	2.7	1.9	3.1	28
1×10^7	3.250	4.2	8.6	5.1	2.2	5.2	46
3×10^7	3.755	5.2	11.6	6.9	3.2	6.1	73

Table 13 Comparing the accuracies of classical tail modelling and guided tail modelling for the eight-variable I-beam problem for various target reliability index values

ΔS	Reliability index	% Error in classical tail modelling (1000 simulation)			% Error in guided tail modelling (1000 simulation)	% Error in guided tail modelling (100 simulation)
		ML	LS	Average		
30 000	2.760	5.0	7.1	5.6	2.1	3.7
40 000	3.256	8.9	13.3	8.2	2.7	8.7
50 000	3.726	15.6	20.4	14.0	5.8	16.6

reliability index can be achieved easily by reducing the applied stress or increasing the strength. Here, the mean value of the strength S is increased by a ΔS amount to attain higher reliability index values as listed in Table 13. The reliability index values are computed through MCS with a sample size of 10^8.

The reliability index estimations attained by using the classical tail modelling techniques and guided tail modelling are given in Table 13. For the classical tail models, the threshold value of $F_t = 0.95$ is used and 1000 limit-state calculations are performed. For the guided tail model, two alternatives are considered. First, the number of limit-state evaluations is kept at 1000. It is found that the accuracies of the reliability estimations are improved compared to classical tail modelling. Second, the number of limit-state evaluations is reduced to 100. It is found that the accuracy of reliability index estimations is not jeopardized much, rather the accuracy is also improved when $\Delta S = 30\,000$.

5.3 Additional example 3: a propped cantilever beam under triangular distributed load

In this example, a propped cantilever beam (see Fig. 8) under a triangular distributed load is examined. The limit-state function for this problem is formulated as the difference between the maximum allowable deflection $(v_{max})_{allow}$ and the maximum deflection of the beam v_{max} due to the applied triangular distributed load given by

$$Y = (v_{max})_{allow} - |v_{max}| \tag{17}$$

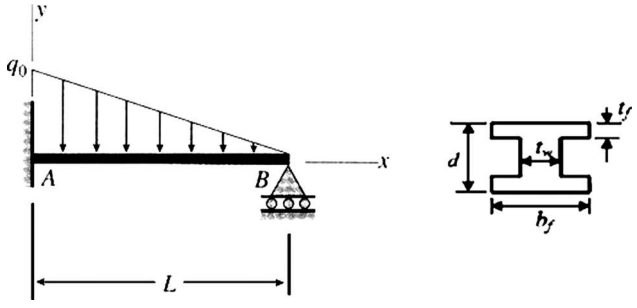

Fig. 8 Cross-section and triangular distributed loading on the propped cantilever beam

Table 14 Mean and standard deviation values of the random variables for the propped cantilever beam problem

Random variable	Mean; standard deviation
q_0 (kN/m)	20; 2
L (m)	6; 0.3
E (GPa)	210; 10
d (cm)	25; 0.5
b_f (cm)	25; 0.5
t_w (cm)	2; 0.2
t_f (cm)	2; 0.2

Note that all random variables follow normal distribution.

The deflection of the beam at any location x can be found from

$$v(x) = -\frac{q_0 x^2}{120LEI}(4L^3 - 8L^2x + 5Lx^2 - x^3) \tag{18}$$

It can be found that the maximum deflection occurs at $x = 0.5528L$ (that is, $v_{max} = v(0.5528L)$). The moment of inertia (I) of the beam can be found from equation (16) as the cross-section of the beam is the same as that of the eight-variable I-beam (see section 5.2). Note that this example problem is more complex than the previous example problems analysed.

In this problem, there are seven random variables following normal distribution with mean and standard deviation values provided in Table 14. The maximum allowable deflection $(v_{max})_{allow}$ is altered within 4–5 mm to attain reliability index values as listed in Table 15. The reliability index values are computed through MCS with a sample size of 10^8.

The reliability index estimations attained by using the classical tail modelling techniques and guided tail modelling are given in Table 15. For the classical tail models, the threshold value of $F_t = 0.95$ is used and 1000 limit-state calculations are performed. For the guided tail model, two alternatives are considered. First, the number of limit-state evaluations is kept at 1000. It is found that the accuracies of the reliability estimations are improved compared to the classical tail modelling. Second, the number of limit-state evaluations is reduced to 100, and it is found that the reliability index estimations have similar accuracy to the classical tail modelling.

Table 15 Comparing the accuracies of classical tail modelling and guided tail modelling for the propped cantilever beam problem for various target reliability index values

v_{max} (mm)	Reliability index	% Error in classical tail modelling (1000 simulation)			% Error in guided tail modelling (1000 simulation)	% Error in guided tail modelling (100 simulation)
		ML	LS	Average		
4.0	2.980	8.4	9.0	7.4	2.4	6.9
4.5	3.503	13.4	16.8	12.5	4.1	14.2
5.0	3.974	17.5	22.9	15.3	9.6	18.2

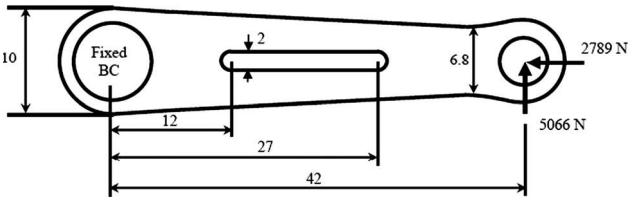

Fig. 9 Loading and boundary conditions for the torque arm. Dimensions are in centimetre [Courtesy of reference [**24**]]

5.4 Additional example 4: torque arm design problem

The limit-state functions for the example problems provided so far in the article used functional relationships between the input and output parameters. However, neither the UDR method nor the tail modelling has this restriction. To demonstrate the effectiveness of the guided tail modelling with limit-states without a functional relationship between the input and output parameters, the current example is included.

This example presents the design of an automobile torque arm. The problem was originally presented by Bennett and Botkin [**23**] and investigated by many researchers including Picheny *et al.* [**24**]. The torque arm is under a horizontal of $F_x = -2789\,\text{N}$ and a vertical load of $F_y = 5066\,\text{N}$ (see Fig. 9). The loads are transmitted from a shaft at the right hole, and the left hole is fixed. The torque arm material has Young's modulus of $E = 206.8\,\text{GPa}$, and Poisson's ratio of $\nu = 0.29$. Seven design variables (d_1 through d_7) alter the shape of the torque arm as shown in Fig. 10.

The limit-state function for the torque arm problem is formulated as

$$Y = \sigma_f - \sigma_{max} \tag{19}$$

where σ_f is the failure stress of the torque arm material and σ_{max} is the maximum von Mises stress developed at the torque arm. All the seven design variables (d_1 through d_7), the applied loads (F_x and F_y) and the failure stress are taken as random variables. The statistical properties of the random variables are provided in Table 16.

There is no functional relationship between the input parameters and the stresses developed at the

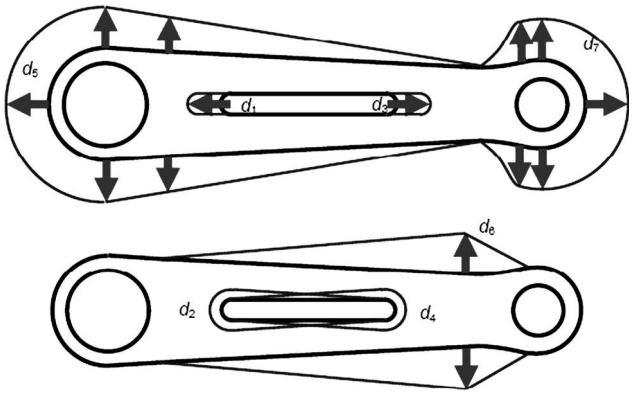

Fig. 10 Design variables used to alter the shape of the torque arm [Courtesy of reference [**24**]]

Table 16 Statistical properties of the random variables for the torque arm problem

Random variable	Distribution type	Mean; standard deviation
d_1 through d_7	Normal	0; 0.1
F_x	Normal	−2789; 278.9
F_y	Normal	5066; 506.6
S	Lognormal	160; 16

control arm. The stresses at the control arm are computed through finite-element analysis by using a MATLAB finite-element toolbox developed by Maute [**25**] and CALFEM [**26**]. Once the stresses at all elements are computed, the maximum stress value is used in equation (19). The mesh density is kept at a low level to allow for repeated analysis required for MCS. Figure 11 depicts the stress distribution on the torque arm when

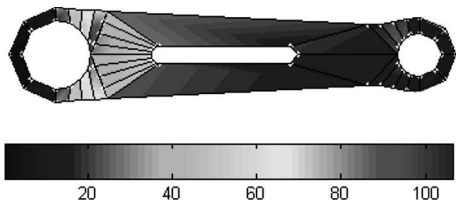

Fig. 11 Von Mises stress distribution on the torque arm when the design variables and the applied loads are assigned to their mean values. Stresses are in MPa

Table 17 Comparing the accuracies of classical tail modelling and guided tail modelling for the torque arm problem for various target reliability index values

Mean σ_f	Reliability index	% Error in classical tail modelling (1000 simulation)			% Error in guided tail modelling (1000 simulation)	% Error in guided tail modelling (100 simulation)
		ML	LS	Average		
160	2.976	5.8	10.8	7.4	1.4	5.9
170	3.439	13.7	14.9	11.0	2.4	9.7
180	3.879	18.0	21.0	13.9	5.7	12.1

the design variables and the applied loads are assigned to their mean values.

Three different target reliability index values are attained by changing the mean value of the failure stress as listed in Table 17. The reliability index values are computed through MCS with a sample size of 10^8.

The reliability index estimations attained by using the classical tail modelling techniques and guided tail modelling are given in Table 17. For the classical tail models, the threshold value of $F_t = 0.95$ is used and 1000 limit-state calculations are performed. For the guided tail model, two alternatives are considered. First, the number of limit-state evaluations is kept at 1000. It is found that the accuracies of the reliability estimations are improved compared to classical tail modelling. Second, the number of limit-state evaluations is reduced to 100. It is found that the accuracy of reliability index estimations is not jeopardized, but the accuracy is also improved compared to classical tail modelling for all the cases considered.

5.5 Comparison of the accuracy of the proposed method with the accuracies of some other reliability assessment methods

In this section, the accuracy of the proposed guided tail modelling is compared with the accuracies of other advanced reliability assessment methods. Since the main motivation of this article is to improve the accuracy and efficiency of the classical tail modelling, the comparison with other reliability assessment methods is not intended to be a thorough one, and so only three other reliability assessment methods are used: the FORM [**27**], augmented advanced mean value method (AMV+ [**28**]), and a UDR-based method (UDR + EGLD [**17**]). Other advanced reliability methods such as SORM [**29**], point estimate methods [**30**], two-point adaptive non-linear approximation method [**31**], expansion methods [**32**], and saddle-point approximation method [**22**] are left out of the comparison.

Tables 18 to 23 present the errors in the predictions of the proposed method, classical tail modelling, FORM, UDR + EGLD, and AMV+ for all example problems provided in the article. The errors are computed relative to reliability index values computed via MCS with 100 million samples. The overall conclusion is that when the limit-state function is linear or has medium non-linearity, the proposed method is not advantageous over the other reliability assessment methods. However, when the limit-state function is highly non-linear, the proposed method as well as the classical tail modelling is more accurate than other reliability assessment methods included in this comparison.

In the comparison of these reliability assessment methods, the number of function evaluations is also important. The classical and the proposed guided tail methods used 1000 function evaluations. The other reliability assessment methods (FORM, UDR + EGLD, and AMV+) are computationally much more efficient in that these methods used one or two orders of magnitude less number of function evaluations for the problems investigated. For the first additional example (i.e. the highly non-linear limit-state) for the reliability index value of 3.755, FORM required 71, UDR + EGLD required 9, and AMV+ required 81 function evaluations. Note that the function evaluations required by FORM and AMV+ depends on the stopping criteria and tolerances used.

6 THE LIMITATIONS OF THE PROPOSED METHOD

The effectiveness of the proposed guided tail modelling depends on the effectiveness of the UDR method and distribution fitting. For instance, if the higher-order interactions between the random variables are strong and the correlations are high, then the accuracy of the UDR method is not very good. In that case, the limit-state function approximations can be performed by using multi-dimensional metamodels instead of the additive decomposition of the UDR method. In addition, the accuracy of y_t prediction will also be a concern, since the UDR will not work well in estimating high probabilities. The error in y_t prediction can be mitigated by choosing a smaller threshold value such as 90 per cent. Note that great caution must be taken while choosing the proper value of the threshold. Choosing a very small threshold yields the distribution not being in the tail region, and hence the theorem of tail equivalence cannot be used. If a very large

Table 18 Errors of various reliability assessment methods for the stress failure mode of Wu's beam problem

Reliabilty index	% Error of the guided tail modelling	% Error of the classical tail modelling	% Error of the FORM	% Error of the UDR + EGLD	% Error of the AMV
3.007	1.3	7.1	0.0	0.1	0.0
3.500	2.4	11.0	0.0	2.5	0.0
4.004	5.7	11.8	0.1	6.5	0.1

Table 19 Errors of various reliability assessment methods for the displacement failure mode of Wu's beam problem

Reliability index	% Error of the guided tail modelling	% Error of the classical tail modelling	% Error of the FORM	% Error of the UDR + EGLD	% Error of the AMV
2.996	1.5	7.8	0.5	1.3	0.8
3.654	3.9	14.5	0.4	0.1	0.8
4.341	13.7	16.2	0.2	4.3	0.8

Table 20 Errors of various reliability assessment methods for the first additional example (a highly non-linear function)

Reliability index	% Error of the guided tail modelling	% Error of the classical tail modelling	% Error of the FORM	% Error of the UDR + EGLD	% Error of the AMV
2.740	1.9	2.4	10.0	28	5.7
3.250	2.2	4.2	7.4	46	5.9
3.755	3.2	5.2	5.4	73	3.1

Table 21 Errors of various reliability assessment methods for the second additional example (eight-variable I-beam design problem)

Reliability index	% Error of the guided tail modelling	% Error of the classical tail modelling	% Error of the FORM	% Error of the UDR + EGLD	% Error of the AMV
2.760	2.1	5.0	2.3	5.3	2.3
3.256	2.7	8.2	1.8	10.4	1.8
3.726	5.8	14.0	1.5	19.1	1.5

Table 22 Errors of various reliability assessment methods for the third additional example (propped cantilever beam under triangular distributed load)

Reliability index	% Error of the guided tail modelling	% Error of the classical tail modelling	% Error of the FORM	% Error of the UDR + EGLD	% Error of the AMV
2.980	2.4	7.4	0.2	15.9	0.2
3.503	4.1	12.5	0.2	22.0	0.2
3.974	9.6	15.3	0.2	31.2	0.2

Table 23 Errors of various reliability assessment methods for the third additional example (torque arm design problem)

Reliability index	% Error of the guided tail modelling	% Error of the classical tail modelling	% Error of the FORM	% Error of the UDR + EGLD	% Error of the AMV
2.976	1.4	5.8	0.5	1.9	0.5
3.439	2.4	11.0	0.5	2.7	0.8
3.879	5.7	13.9	0.5	8.7	1.1

threshold is chosen, on the other hand, the uncertainty in threshold causes large errors.

Similarly, the accuracy of the distribution fitting is also important. The EGLD is suitable for approximating the uni-modal (i.e. single peaked) distributions. If the distribution of the limit-state function is multi-modal, then the threshold value can be computed by using multi-dimensional metamodels within an MCS framework.

The classical tail modelling does not require generating input random samples and propagating them to obtain the output samples. Rather, it only focuses on output samples. For example, if 1000 samples are taken in a non-destructive evaluation of a nuclear reactor, then the tail modelling can be used effectively to estimate the reliability of the reactor. In this case, neither any information on the input random variables, nor any assumption on uncertainty propagation is used. The proposed guided tail modelling method, on the other hand, does require probability distribution of the input random variables for UDR and EGLD. This is a major drawback of the proposed method against classical tail modelling.

7 CONCLUSIONS

The classical tail modelling procedure is based on performing a relatively small number of limit-state calculations through Monte Carlo sampling, then fitting a GPD to the tail part of the data. The limit-state calculations that do not belong to the tail part are discarded. This article proposed an efficient tail modelling procedure based on guiding the limit-state evaluation points so that the limit-state values have high chances of falling into the tail region, and hence the amount of wasted data was reduced. The guidance of the limit-state evaluation points was achieved through a procedure that combines the use of the UDR method and distribution fitting. The efficiency and accuracy of the proposed method was tested through four structural mechanics problems, and it was found that the accuracy of the reliability prediction can be significantly improved by using guided tail modelling compared to the classical tail models for about the same number of limit-state evaluations. Alternatively, the improvement of the accuracy can be traded off for reducing the number of limit-state evaluations. That is, the number of limit-state evaluations can be reduced while keeping the accuracy of the guided tail modelling at the same level with that of the classical tail modelling.

The limit-state functions for the example problems provided in this study were all explicit. However, neither the UDR method nor the tail modelling has this restriction. Going over the procedures of the UDR method and the tail modelling, one can see that these methods can handle implicit limit states. In addition, the capability of the proposed method for system reliability estimation is not discussed in this study. However, the system reliability calculation procedure proposed by Ramu [**12**] using inverse reliability measure based tail modelling can be used easily within the framework of guided tail modelling. System reliability estimation using guided tail modelling is considered to be the subject of a future study.

Even though the guided tail modelling provides efficient and accurate reliability estimations, the accuracy of guided tail model reduces as the reliability index increases. The accuracy of tail models can be improved by using inverse reliability measures in tail models as proposed by Ramu [**12**]. In a future study, the proposed guided tail modelling can be combined with the inverse reliability measure-based tail models for further accuracy improvement.

The major limitations of this study can be summarized as follows: since the guided tail modelling is based on the UDR method and distribution fitting, the limitations of these two applies to the guided tail modelling. For instance, if the higher-order interactions between the random variables are strong and the correlations are high, then the accuracy of the UDR method is questionable. In that case, more accurate models for limit-state function estimation and statistical moment estimation should be used. Similarly, if the distribution of the limit-state function is multi-modal, the EGLD that can only mimic uni-modal distributions will not be useful. In that case, more advanced distribution fitting techniques should be utilized. Finally, the classical tail modelling does not require generating input random samples and propagating them to obtain the output samples, rather it only focuses on output samples. However, the guided tail modelling method does require probability distribution of the input random variables for utilizing UDR and EGLD.

ACKNOWLEDGEMENT

The funding provided by the TUBITAK under Grant No. MAG-109M537 is gratefully acknowledged.

REFERENCES

1 **Melchers, R. E.** Importance sampling in structural systems. *Struct. Safety*, 1989, **6**, 3–10.

2 **Wu, Y. T., Shin, Y., Sues, R.,** and **Cesare, M.** Safety-factor based approach for probability-based design optimization. In Proceedings of the 42nd AIAA/ASME/ASCE/AHS/ASC Structures, Structural Dynamics, and Materials Conference, Seattle, WA, 16–19 April 2001, paper no. AIAA-2001-1522.

3 **Nie, J.** and **Ellingwood, B. R.** Directional methods for structural reliability analysis. *Struct. Safety*, 2000, **22**, 233–249.

4 **Castillo, E.** *Extreme value theory in engineering*, 1988 (Academic Press, San Diego, CA).

5 **Caers, J.** and **Maes, M.** Identifying tails, bounds, and endpoints of random variables. *Struct. Safety*, 1998, **20**, 1–23.

6 **Kim, N. H., Ramu, P.,** and **Queipo, N. V.** Tail modeling in reliability-based design optimization for highly safe structural systems. In Proceedings of the 47th AIAA/ASME/ASCE/AHS/ASC Structures, Structural Dynamics, and Materials Conference, Newport, RI, 2006, AIAA paper 2006-1825.

7 **Ramu, P., Kim, N. H., Haftka, R. T.,** and **Queipo, N.V.** System reliability analysis and optimization using tail modeling. In Proceedings of the 11th AIAA/ISSMO Multidisciplinary Analysis and Optimization Conference, Portsmouth, VA, 2006, AIAA paper 2006-7012.

8 **Rahman, S.** and **Xu, H.** A univariate dimension-reduction method for multi-dimensional integration in stochastic mechanics. *Probab. Eng. Mech.*, 2004, **19**, 393–408.

9 **Maes, M. A.** and **Breitung, K.** Reliability-based tail estimation. In Proceedings of the IUTAM Symposium on *Probabilistic structural mechanics (advances in structural reliability methods)*, San Antonio, TX, June 1993, pp. 335–346.

10 **Boos, D.** Using extreme value theory to estimate large percentiles. *Technometrics*, 1984, **26**(1), 33–39.

11 **Hasofer, A.** Non-parametric estimation of failure probabilities. In *Mathematical models for structural reliability* (Eds F. Casciati and B. Roberts), 1996, pp. 195–226 (CRC Press, Boca Raton, FL).

12 **Ramu, P.** *Multiple tail models including inverse measures for structural design under uncertainties*. PhD Thesis, University of Florida, Gainesville, FL, 2007.

13 **Freimer, M., Mudholkar, G., Kollia, G.,** and **Lin, C.** A study of the generalized tukey lambda family. *Commun. Stat. – Theory Methods*, 1988, **17**(10), 3547–3567.

14 **Karian, Z. E., Dudewicz, E. J.,** and **McDonald, P.** The extended generalized lambda distribution system for fitting distributions to data: history, completion of theory, tables, applications, the 'final word' on moment fits. *Commun. Stat. – Comput. Simul.*, 1996, **25**(3), 611–642.

15 **Lakhany, A.** and **Mausser, H.** Estimating the parameters of the generalized lambda distribution. *Algo Res. Q.*, 2000, **3**(3), 47–58.

16 **Fournier, B., Rupin, N., Bigerelle, M., Najjar, D., Iost, A.,** and **Wilcox, R.** Estimating the parameters of a generalized lambda distribution. *Comput. Stat. Data Anal.*, 2007, **51**, 2813–2835.

17 **Acar, E., Rais-Rohani, M.,** and **Eamon, C.** Reliability estimation using univariate dimension reduction and extended generalized lambda distribution. *Int. J. Reliab. Safety*, 2010, **24**(2/3), 166–187.

18 **Ramu, P., Kim, N. H.,** and **Haftka, R. T.** Error amplification in failure probability estimates of small errors in surrogates. In Proceedings of the World Congress, Detroit, MI, 16–19 April 2007, paper no. 2007-01-0549, SAE-2007.

19 **Qu, X.** and **Haftka, R. T.** Reliability-based design optimization using probabilistic sufficiency factor. *Struct. Multidiscip. Optim.*, 2004, **27**(5), 314–325.

20 **Ba-abbad, M. A., Nikolaidis, E.,** and **Kapania, R. K.** New approach for system reliability-based design optimization. *AIAA J.*, 2006, **44**(5), 1087–1096.

21 **Goldstein, A. A.** and **Price, J. F.** On descent from local minima. *Math. Comput.*, 1971, **25**(115), 569–574.

22 **Huang, B.** and **Du, X.** Uncertainty analysis by dimension reduction integration and Saddlepoint approximations. *J. Mech. Des.*, 2006, **126**(1), 26–33.

23 **Bennett, J. A.** and **Botkin, M. E.** *The optimum shape*, 1986 (Plenum Press, New York, NY).

24 **Picheny, V., Kim, N. H., Haftka, R. T.,** and **Quiepo, N. V.** Conservative predictions using surrogate modeling. In Proceedings of the 49th AIAA/ASME/ASCE/AHS/ASC Structures, Structural Dynamics, and Materials, Schaumburg, IL, April 2008.

25 **Maute, K.** *Design element toolbox*, 2009 (Center for Aerospace Structures, University of Colorado, Boulder, CO).

26 CALFEM. *A finite element toolbox to MATLAB*, version 3.3, 1999 (Structural Mechanics and Solid Mechanics, Lund University, Lund, Sweden).

27 **Hasofer, A. M.** and **Lind, N. C.** Exact and invariant second-moment code format. *J. Eng. Mech. Div.* ASCE, 1974, **100**, 111–121.

28 **Wu, Y. T.** Computational methods for efficient structural reliability and reliability sensitivity analysis. *AIAA J.*, 1994, **32**(8), 1717–1723.

29 **Neumann, H. J., Fiessler, B.,** and **Rackwitz, R.** Quadratic limit states in structural reliability. *J. Eng. Mech.*, 1979, **105**(4), 661–676.

30 **Rosenblueth, E.** Two-point estimates in probability. *Appl. Math. Model.*, 1981, **5**, 329–335.

31 **Xu, S.** and **Grandhi, R. V.** Multi-point approximation for reducing the response surface model development cost in optimization. In Proceedings of the 1st ASMO UK/ISSMO Conference on *Engineering design optimization*, West Yorkshire, UK, 8–9 July 1999, pp. 381–388.

32 **Kim, N. H., Wang, H.,** and **Queipo, N. V.** Efficient shape optimization under uncertainty using polynomial chaos expansions and local sensitivities. *AIAA J.*, 2006, **44**(5), 1112–1116.